



Timescales and dynamics of the formation of a thermocline

Giulio Boccaletti*

Atmospheric and Oceanic Sciences Program, Princeton University, Princeton, NJ, USA

Received 5 December 2003; accepted 5 October 2004
Available online 30 November 2004

Abstract

In a state of equilibrium, the constraint of a balanced heat budget for the ocean strongly influences the depth of the tropical thermocline because that depth controls the rate at which the ocean absorbs heat from the atmosphere. Thus, an increase in the oceanic heat loss in high latitudes results in a shoaling of the equatorial thermocline so that the heat gain also increases. How does the ocean adjust to such a new equilibrium state after an abrupt change in the heat flux in high latitudes? The adjustment of the wind-driven circulation of the upper ocean is shown to involve two timescales. The first is the familiar adiabatic wave-adjustment time associated with the horizontal redistribution of warm water above the thermocline in shallow water models. (This is essentially the time it takes Rossby and Kelvin waves to propagate from the disturbed extra-equatorial region to the equator.) The second adjustment-time is associated with the diabatic processes that come into play once the waves from higher latitudes modify the thermal structure in low latitudes and hence the flux of heat into the ocean; it is the timescale on which the ocean recovers a balanced heat budget. The identification of this timescale is the main result of this paper.

Through a series of simulations of an idealized ocean basin, we identify the diabatic timescale and argue that it is determined by the strength of the upwelling and the intensity of the air–sea heatfluxes. By simulating the formation of a thermocline from isothermal conditions, we are able to relate this timescale to other relevant timescales such as that associated with diffusive processes and the adiabatic timescale invoked by Gu and Philander [Gu, D., Philander, S.G.H., 1997. Interdecadal

* Present address: Department of Earth, Atmospheric and Planetary Sciences, Massachusetts Institute of Technology, Cambridge, MA 02139-4307, USA.

E-mail address: gbocca@mit.edu.

climate fluctuations that depend on exchanges between the tropics and extra-tropics. *Science* 275, 805–807].

© 2004 Elsevier B.V. All rights reserved.

Keywords: Thermocline; Ocean circulation; Ocean waves; Thermohaline circulation

1. Introduction

The circulation that maintains the thermal structure of the ocean has two main components: a deep, slow overturning circulation, and a shallow, rapid, wind-driven circulation associated with the ventilated thermocline (Luyten et al., 1983). The latter component involves the subduction of surface water in certain extra-tropical regions, whereafter the water travels to the equator, to appear there on the order of a decade later. If anomalously warm water (say) were subducted, it would in due course affect the structure of the equatorial thermocline and hence ocean–atmosphere interactions. Gu and Philander (1997) invoked such reasoning to argue that decadal variability in low latitudes could have its origin in high latitudes. Thus far, evidence for the advection of subducted anomalously warm or cold water all the way to the equator is absent from the analyses of measurements (Deser and Blackmon, 1995; Schneider et al., 1999), and also in studies with oceanic GCMs (Lysne et al., 1997; Hazeleger et al., 2001). However, studies of passive tracers such as tritium (Fine et al., 1987; McPhaden and Fine, 1988) confirm that the wind-driven circulation does connect the tropics and extra-tropics. Why does that circulation fail to advect anomalously warm water all the way to the equator?

The appearance of anomalously warm water at the surface in the extra-tropics can be interpreted as a perturbation to the oceanic heat budget which involves the gain of heat, mostly in low latitudes, especially equatorial upwelling zones, and the loss of heat, mostly in high latitudes, especially where cold air moves from continents onto relatively warm currents such as the Gulf Stream and Kuroshio. To ensure a balance between the gain and loss—a necessary condition in a state of equilibrium—the oceanic circulation transports heat from low to high latitudes. In doing so, the circulation maintains the oceanic thermal structure whose salient feature is a remarkably sharp and shallow thermocline in the tropics. (If the heat gained in the equatorial upwelling zones were not carried away by the currents, the equatorial thermocline would deepen very rapidly.) Boccaletti et al. (2004) quantify the idea that the constraint of a balanced heat budget for the ocean controls the depth of the equatorial thermocline. They demonstrate by means of numerical models of the ocean how a change in the oceanic heat loss in high latitudes is accompanied by a corresponding change in the heat gain in low latitudes where the depth of the thermocline changes. (The shallower the equatorial thermocline, the more heat that part of the ocean absorbs and exports poleward.) These results are for steady-state conditions and therefore raise the obvious question: what is the temporal evolution of the oceanic adjustment to an instantaneous change in the boundary conditions at the ocean surface?

Previous studies that are relevant to these questions have concerned mainly the adiabatic oceanic adjustment to changes in the surface winds. These studies (see Philander, 1990)

have established that the adiabatic adjustment depends critically on oceanic Rossby and Kelvin waves. The same waves are also of vital importance to the adjustment of shallow water models of the ocean to specified sources and sinks of water (Cane and Sarachik, 1979; Kawase, 1987). These results provide an answer to the question raised at the end of the first paragraph above. A disturbance in the form of anomalously warm (cold) water at the surface in the extra-tropics will disperse into waves, with greater and greater efficiency the lower the latitude. The waves therefore atrophy the signal, the anomalously warm water, as it is advected equatorward. This adiabatic wave-adjustment is an important part of the response to a change in the heat flux at the surface, but there is more to the story of the diabatic adjustment. The fact that the anomalous water is dispersed does not by itself determine the time evolution of the heatflux at the surface. Therefore, a problem remains: advection cannot be invoked to determine the timescale over which the tropics and the extra-tropics are connected, as waves disperse the signals before they reach the tropics. What determines the timescale of that connection?

The main result from the calculations to be presented here is that the adjustment of the upper ocean to a change in surface heat fluxes involves two timescales. The first is the familiar wave propagation time τ_w , the time it takes for waves to propagate to the equator from the extra-tropical region where the disturbance is introduced. This relatively rapid phase of the adjustment permits an extra-equatorial disturbance to influence the depth of the equatorial thermocline. The second phase of the adjustment occurs over a timescale τ_d that depends on the diabatic processes involved in the oceanic heat gain. This diabatic timescale ultimately controls the timescale of the response.

The structure of the paper is as follows. Section 2 describes the model used in this study.

In Section 3, we consider the first idealized case in which a circulation in a closed ocean basin maintains a thermocline by transporting heat from the region of heat gain in low latitudes to the region of heat loss in high latitudes. Following Haney (1971), we impose a heat flux of the form

$$Q = \alpha(T^* - T) \quad (1)$$

where α is a constant, T the sea surface temperature and T^* is an effective atmospheric temperature. T^* is chosen to be 25 °C in the tropics and to linearly decrease to 10 °C in the extra-tropics. A perturbation in the heatflux is introduced in the extra-tropics and the adjustment to a new steady state is analyzed. This experiment is in many ways similar to previous adjustment studies (Godfrey, 1975; Cane and Sarachik, 1979; Kawase, 1987); it treats a perturbation on an existing stratification, but the focus on the heat budget allows us to shed new light on the problem.

As argued in Boccaletti et al. (2004), diabatic processes are ultimately responsible for controlling the thermal structure. The associated timescale is not only relevant to describe the response of the ocean to perturbation, but also to characterize the time it takes to control the absolute depth of the thermocline. Nowhere is this more clear than in the case in which a thermocline is created where none was present. In Sections 4 and 5, we present experiments targeted at examining this non-linear process.

In Section 4, a motionless ocean, initially at a uniform temperature of 10 °C, is forced, from time $t=0$ onwards, with spatially uniform easterly winds and a heat flux of the form

(1), but where now $T^* = 25^\circ\text{C}$ everywhere. The ultimate state of affairs is obvious: the ocean will again be isothermal, at a temperature $T = 25^\circ\text{C}$. (The vertical walls and flat ocean floor are assumed to be non-conducting.) By analysing the development and ultimate dissipation of the stratification, this experiment allows us to identify all processes responsible for controlling the thermocline and their associated timescales.

In Section 5, we describe experiments corresponding to a case in which the initial condition is again a 10°C isothermal ocean but now both warming and cooling occur. Rather than restoring towards a temperature T^* with a constant value, we allow T^* to vary with latitude so that it is 25°C between 12°N and 12°S , and tapers linearly to 10°C from 12° latitude to the northern and southern boundaries, as in the first perturbation experiment. This change allows the ocean to gain heat across its surface in low latitudes, and to lose heat across the surface in higher latitudes. The constraint of a balanced heat budget, which in the problem with isothermal forcing could be satisfied only locally, at every point, when the surface temperature everywhere is 25°C , can now be satisfied non-locally by transporting heat from regions of heat gain to regions of heat loss.

While this study is concerned mainly with the adjustment of the upper ocean, rather than that of the deep ocean below the thermocline, this set of simulations allows us to point out the relationship between upper ocean processes and the diffusive ones that control the abyss.

Section 6 presents a discussion and conclusions.

2. The model setup

A small tropical basin is forced by uniform easterly winds and an idealized thermal boundary condition. The basin extends from 16°N to 16°S and is 40° wide. The choice of such a small basin is made to allow a large number of cases to be run.

For these initial experiments, the constant wind strength is 0.05 Pa , and the complication of a full gyre circulation and boundary current is largely avoided. Winds force upwelling within a Rossby radius of the equator and drive surface Ekman flow towards the southern and northern boundaries. The convergence of Ekman flow, due to the sphericity of the Earth, produces an equatorward flow which balances the Ekman flow in the mixed layer, so that the circulation is approximately zonally symmetric. This symmetry obviously breaks down at the equator, where the easterly winds force an east–west tilt in the thermocline.

The heat flux is $(T^* - T) \times 50\text{ W/m}^2$ and restores the surface temperature T to a specified T^* (Haney, 1971). We consider experiments with constant $T^* = 25^\circ\text{C}$ and with latitudinally varying T^* . In the latter case, T^* is 25°C between 12°N and 12°S and linearly tapered to 10°C at the northern and southern boundaries.

The model used is the GFDL MOM 4. Horizontal resolution is specified as $1/2^\circ$ everywhere, with 32 levels in the vertical. The vertical resolution is 10 m in the upper 200 m . For simplicity, salinity is constant throughout the basin so that temperature is the only active tracer. The initial temperature is everywhere 10°C , unless otherwise specified. Vertical mixing is the Pacanowski and Philander (1981) scheme solved using a maximum vertical mixing coefficient of $50 \times 10^{-4}\text{ m}^2/\text{s}$ and a background diffusivity of $0.01 \times 10^{-4}\text{ m}^2/\text{s}$, un-

less otherwise specified. Constant lateral mixing coefficients are $A_m = 2.0 \times 10^3 \text{ m}^2/\text{s}$ and $A_h = 1.0 \times 10^3 \text{ m}^2/\text{s}$ for momentum and heat, respectively.

3. The linear perturbation problem

Consider first the case in which a thermocline already exists, and it is perturbed by altering the surface heat budget. The basic state for this experiment is shown in Figs. 1 and 2. This is a case in which T^* is allowed to vary latitudinally. The uniform winds produce an Ekman flow which advects warm tropical water poleward. When this warm water encounters the cold restoring temperature, beyond 12° latitude, it is cooled and subducted. Water then returns at depth towards the equator, where it is upwelled and warmed in a cold tongue. The heat flux pattern shown in Fig. 2 reflects this circulation. In steady state, the thermal structure produced by this idealized experiment resembles in many ways the observed thermocline (Fig. 1): the equatorial stratification is tilted in response to the easterly winds, and the eastern portion of the thermocline outcrops producing the cold tongue, a reasonably deep lens of warm water overlies the cold abyss, and the circulation is the combination of a wind-driven meridional flow and of a deeper diffusively driven flow.

To perturb this basic state, we change the high latitude restoring temperature from 10°C to 15°C , thus suddenly decreasing the heat loss. The easterly winds now drive 25°C water into a region where the restoring temperature gradient is lower than it used to be. In the unperturbed tropics, initially nothing changes: the local boundary conditions, equatorward of 12° latitude, are the same as before. However, this state of affairs cannot persist. The high latitude heat loss has decreased, while the tropical warming is left unchanged; a net heating results which necessarily must lead to an increase in the amount of warm water. This additional warm water is redistributed over the entire basin, thus leading to a change in stratification everywhere, including the tropics. As the warm water increases, the thermocline deepens, the cold tongue shrinks, and the heat gain is reduced, driving the ocean towards a new balanced state, where heating and cooling are once again in balance (Boccaletti et al., 2004a,b). How long does it take for the tropical thermocline to feel the high latitude change? How long for the system to reach a new equilibrium?

The first question is straightforward and has been the subject of a number of studies (e.g. Kawase, 1987; Cane, 1989; Yang, 1999; Johnson and Marshall, 2002). The modification of the high latitude restoring temperature T^* results in an initial accumulation of warm water. This accumulation in turn leads to an adjustment in which a boundary signal leaves the high latitudes, travels along the western boundary, across the equator, and up the eastern boundary. There, it sheds a Rossby front that crosses the basin, completing the adjustment. The equator “feels” the modification once the fastest wave has arrived, while the subtropics respond in the wake of the Rossby front. The vertical structure of the anomaly resembles a first baroclinic mode on the existing stratification (Philander, 1990), and—if the amplitude of this signal is very small—the waves obey linear dynamics. Overall, the tropical region is first affected by the high latitude change in under 6 months, although—depending on the size of the basin—the adjustment of the midlatitude thermocline can be much slower.

Boundary waves are considerably faster than Rossby waves, so that in practice, the wave adjustment process is associated with a timescale τ_w , determined by the crossing time of the

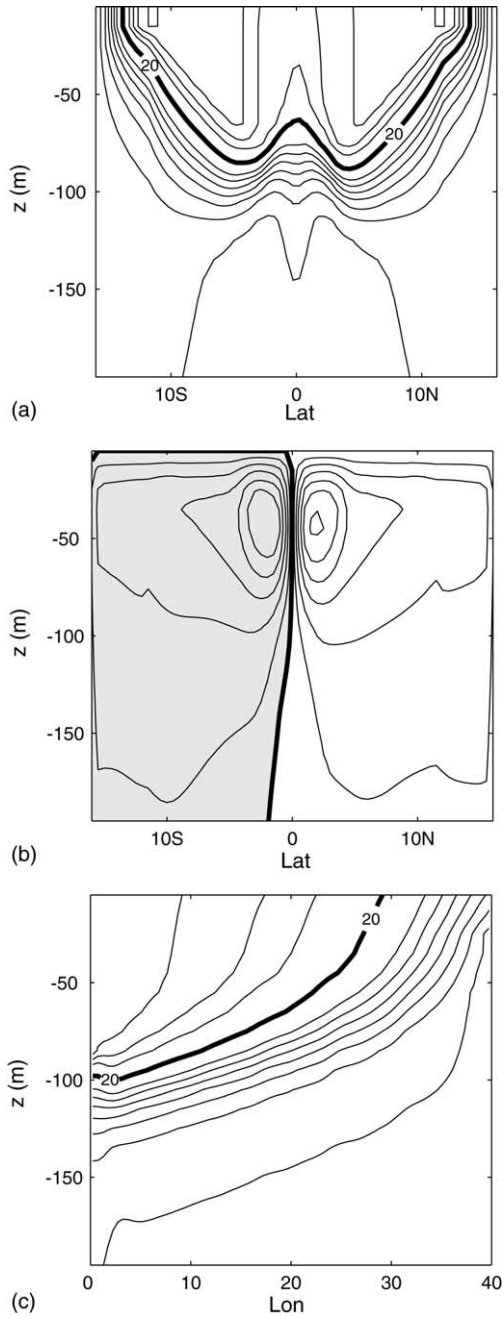


Fig. 1. Mean structure of the steady-state solution for a small basin. (a) Meridional section of temperature at 20° longitude. Contour interval is 2°C . (b) Meridional overturning streamfunction. Contour interval 2.5 Sv. Shaded area corresponds to negative values. (c) Equatorial thermal structure. Contour interval is 2°C .

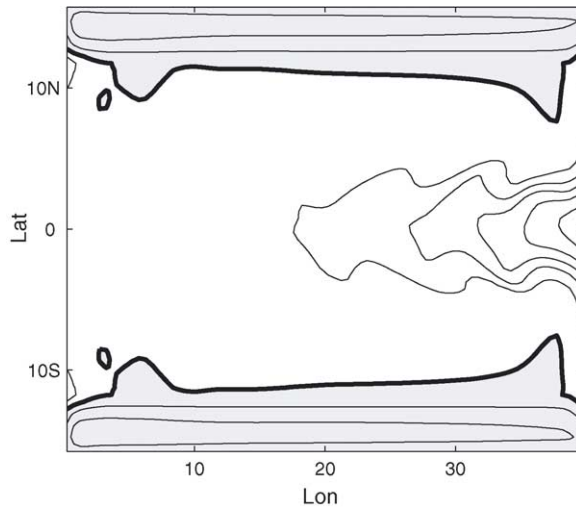


Fig. 2. Mean structure of the steady-state solution for a small basin. Surface heat flux, contour interval is 50 W/m^2 . Shaded area corresponds to negative values.

basin by the Rossby signal. [Johnson and Marshall \(2002\)](#) solved analytically a problem for a shallow water basin in which this is the only relevant timescale. In that study, the basin is forced by a source at the northern boundary, the water floods the basin in the way described above, and is then removed by a geostrophic flow at the southern boundary. The outflow is proportional to the depth of the eastern boundary thermocline at the southern end, and equilibrium is reached when the rate at which water flows out of the southern boundary equals that of the mass source. Because the outflow accommodates the perturbation through geostrophic adjustment accomplished by Rossby waves, the response is governed by a delay equation with lag τ_w ([Johnson and Marshall, 2002](#)).

The case presented by [Johnson and Marshall \(2002\)](#) is meant to illustrate the response of the Atlantic meridional overturning circulation and is ill-suited to represent the response of the wind driven circulation because of the substantially different mass budget. When the subtropical cooling associated with subducting water is suddenly decreased, it is warm water originating in the tropics that starts accumulating. However, unlike the southern outflow in [Johnson and Marshall \(2002\)](#), the response of the tropics is not governed solely by wave adjustment. The excess warm water, which is produced at the equator and transported poleward by the Ekman flow, can no longer be accommodated by the cooling and is returned to the equator as boundary and Rossby waves. As a result, the tropical thermocline deepens, the cold tongue is reduced, the heating is reduced, and the net contribution of warm water is decreased. This process continues until the source (equatorial upwelling) and sink (subtropical cooling) are in balance again. While the communication between source and sink is governed by wave dynamics, the adjustment of the source is no longer governed by wave adjustment alone. Rather, it ultimately depends on the rate at which the mean depth of the thermocline can change. This is in turn a function of wind-driven entrainment (which determines the rate at which cold water is ex-

posed to the surface) and surface heating (which determines how fast that water can be warmed).

We can quantify the adjustment of the mean thermocline depth D as

$$D_t \sim w_e \frac{h}{D} \quad (2)$$

where w_e is the strength of the wind-driven upwelling, h the depth of the mixed layer, and for the time being, we have ignored the effects of diffusion. Expression (2) is based on a model introduced in Boccaletti et al. (2004), where it was assumed that entrainment of water into the surface layer is inversely proportional to the depth of the thermocline D and directly proportional to the strength of the tropical Ekman upwelling w_e . When $D = h$, the depth of the mixed layer, the entrainment is maximum and equal to w_e . When $D \rightarrow \infty$, the entrainment is zero. This simple expression captures the essence of the relationship between thermocline depth and entrainment of subthermocline waters (Boccaletti et al., 2004a,b). From Eq. (2), it follows that the timescale for the deepening of the thermocline is:

$$\tau_d \sim \frac{D^2}{w_e h}. \quad (3)$$

However, τ_d is a diabatic timescale related to strictly diabatic processes of water mass transformation. This becomes evident by estimating the scale D for the depth of the thermocline from the heat budget, as done in Boccaletti et al. (2004) (their Eq. (11)):

$$Q = w_e \frac{h}{D} \Delta T. \quad (4)$$

A relationship between the timescale and the parameters responsible for the diabatic processes can be then determined:

$$\tau_d \sim w_e \frac{h}{Q^2 / \Delta T^2}. \quad (5)$$

For $w_e \sim 0.5 \times 10^{-5}$ m/s, $h \sim 50$ m, $\Delta T \sim 15^\circ\text{C}$ and $Q \sim 100 \text{ W/m}^2 / (\rho C_p) \sim 5 \times 10^{-5} \text{ }^\circ\text{C m s}^{-1}$, we have a timescale of about 2 years.

This estimate agrees with the numerical simulation of Fig. 3, which shows the time evolution of the heat source and sink, averaged over the tropical and boundary regions, respectively. Despite the rapidity of the Kelvin waves, and the complicated picture offered by wave dynamics, the thermocline deepens gradually and the system adjusts smoothly to the new state. The heat budget perspective offers a simple picture: the perturbed heat sink in the subtropics behaves almost as a step function, after a very brief initial adjustment; the equatorial heat-flux decreases gradually, as the rate of transformation adjusts.

From the point of view of the heat budget, waves are just the process by which mass is redistributed. What determines the time τ_d of thermocline deepening is the net heating of the basin, which depends on the boundary condition and on the intensity of the wind-driven circulation. Water is added at a rate that depends on the imbalance between heating and cooling, and the imbalance is reduced as the thermocline reaches a new mean state in which the heating and cooling are equal and opposite. In the next section, we shall further illustrate the relationship between waves, which introduce a transient time τ_w , and the

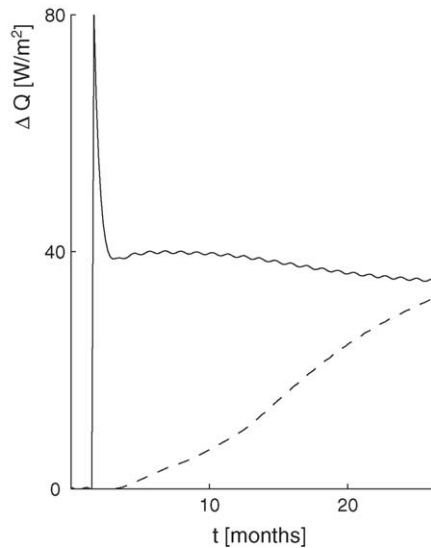


Fig. 3. Response of the heat budget to an imposed cooling anomaly, obtained by instantaneously changing the high latitude restoring temperature from 10°C to 15°C . Plot of the time evolution of the heat anomaly in the region of heating (dashed, averaged over $[-4^{\circ}, 4^{\circ}]$), and cooling (solid, averaged elsewhere). The anomalous heating is multiplied by -1 for ease of comparison.

diabatic adjustment governed by τ_d . So far, we have ignored open-ocean mixing, which is also responsible for transforming water masses. Its relationship to τ_d is also addressed in the next section.

4. The formation of a thermocline

The formation of a thermocline from isothermal conditions offers a useful setting in which we can compare the effects of diabatic and dynamical processes. Consider first the simplest case of an isothermal basin, initially at 10°C , subject to a uniform restoring towards $T^* = 25^{\circ}$ applied to its surface. Thermal and wind forcing are applied at the same time and Figs. 4 and 5 show snapshots of meridional sections and streamfunctions at different times after the forcing has been turned on.

The final state of such a simulation is obvious: because there is no cooling, the basin will have to ultimately reach a uniform temperature of 25°C everywhere. However, the processes involved in reaching that final state have significantly different timescales, allowing us to discriminate between them.

The surface layer initially warms on a timescale proportional to α^{-1} (where α is the restoring coefficient). At the same time, easterly winds accelerate zonally the flow. On timescales greater than inertial (f^{-1}), rotation becomes important and the flow redirects meridionally. This state of affairs leads to vigorous upwelling around the equatorial region and convergence off the equator.

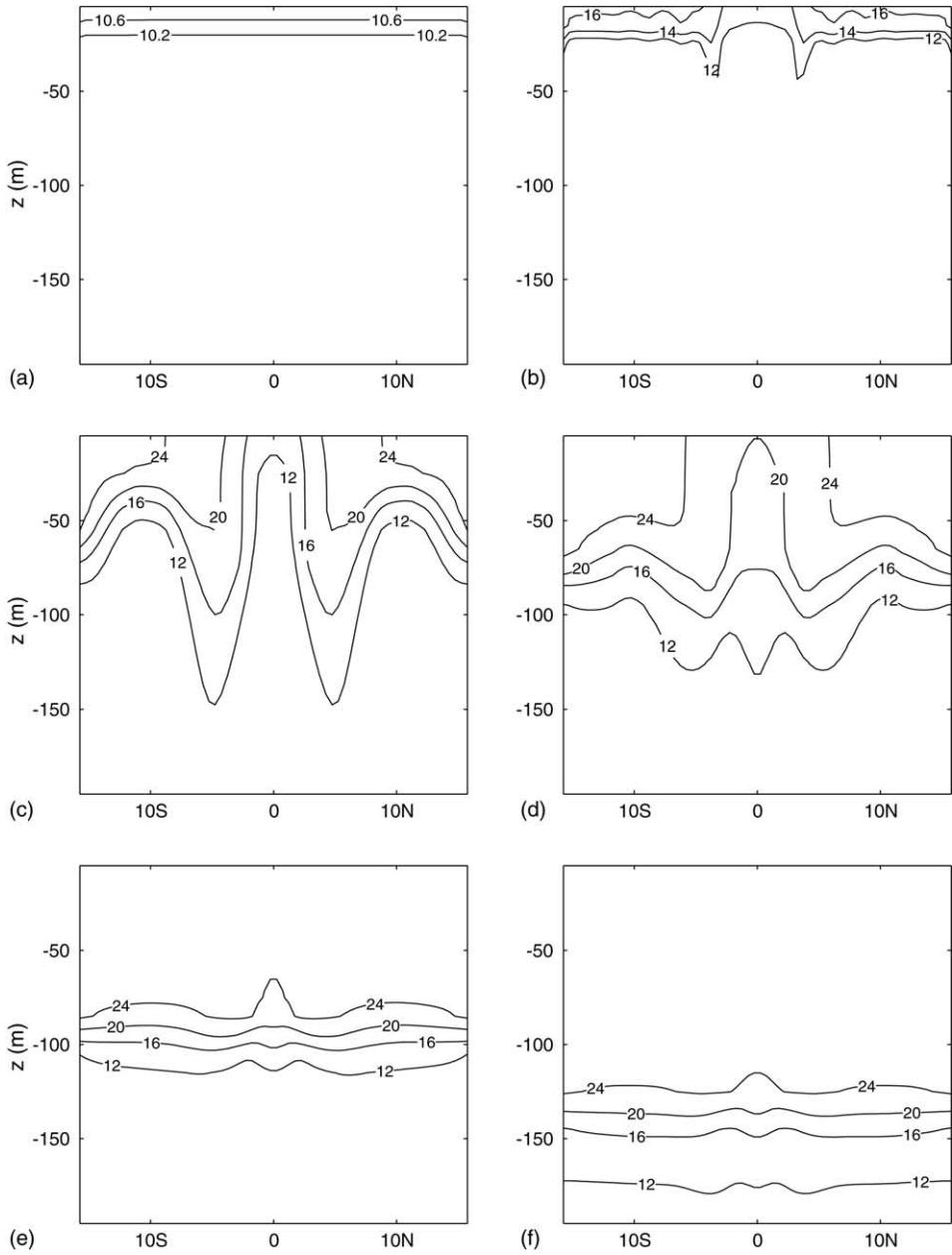


Fig. 4. Sequence of sections in the middle of the basin during the adjustment from isothermal conditions, after 1 day (a), 10 days (b), 150 days (c), 350 days (d), 1000 days (e), 10,000 days (f).

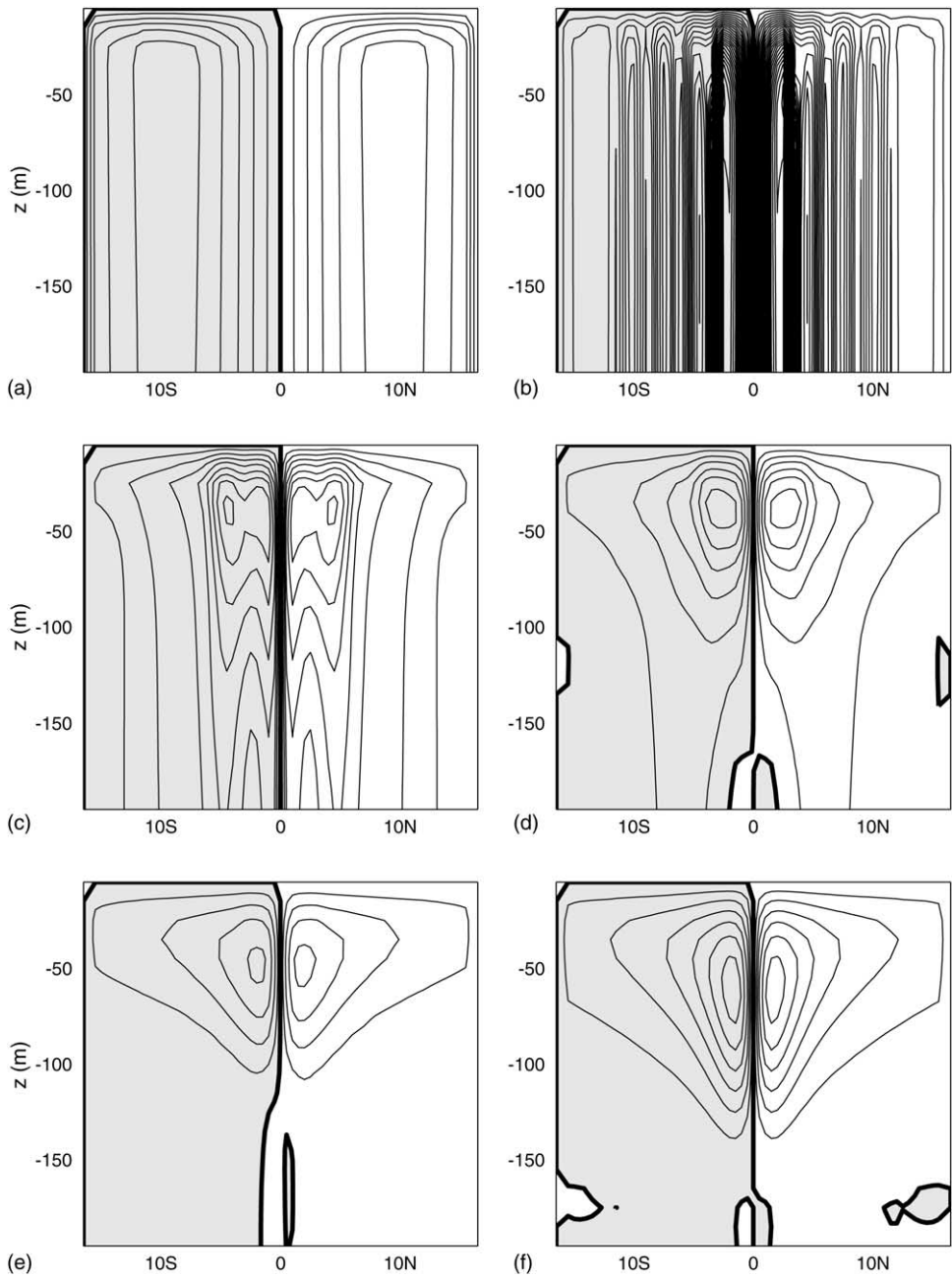


Fig. 5. Sequence of meridional overturning streamfunctions. The panels correspond to those of Fig. 4. Contour interval is 2.5 Sv.

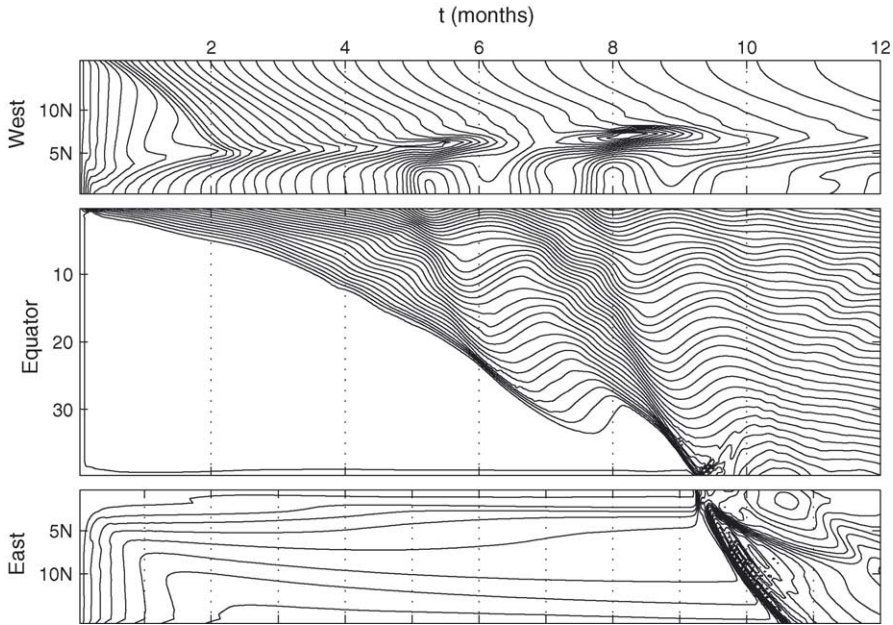


Fig. 6. Adjustment of the averaged temperature structure along the perimeter of the domain for the first year of simulation. The domain, initially isothermal, is restored towards a uniform 25 °C. Contour interval is 1 °C.

Contour interval is 25 Sv. This first part of the adjustment can be seen in the top panels of Figs. 4 and 5. During this phase, cold water is being upwelled at the equator and heated by the restoring boundary condition. It flows poleward and is converged off the equator.

A thermocline is formed as a thermal boundary layer between the warming surface waters and the abyss. It is initially zonally symmetric, much as would happen in a channel on a rotating sphere. However, because of the boundaries, the zonal symmetry is lost in the wake of geostrophic adjustment. The boundary and interior wave adjustment is of the type described, for instance, in Cane and Sarachik (1979) (see also Kawase, 1987; Anderson and Gill, 1975), although it is important to note that in our case, the process is different from those studies, for the simple reason that the stratification is being formed as the front propagates (Stern, 1980; Griffiths, 1986; Hellfrich et al., 1999).

Fig. 6 shows the average temperature along the perimeter of the basin as a function of time, which highlights the qualitative similarity with the well-known boundary adjustment of the linear studies (Philander, 1990). Initially, the thermocline deepens uniformly along the western and eastern boundaries, as a result of the off-equatorial convergence of warm water by a largely zonally symmetric circulation. The deepening is however interrupted by propagating boundary signals originating from the high latitudes along the western boundary and from the equator along the eastern boundary. These signals carry the signature of the geostrophic adjustment of the boundaries. At the same time, a front originating from the western side of the equator crosses the basin in about 9 months, after which time it reaches the eastern boundary and propagates poleward. This is the non-linear analogue of

the customary equatorial Kelvin wave (Philander, 1990). During the poleward propagation, a Rossby front propagates towards the interior establishing the east–west asymmetry. This phase of the adjustment corresponds to the middle panels of Figs. 4 and 5. After about a year, the wave adjustment ends, the flow is in geostrophic equilibrium, and the circulation satisfies Sverdrup balance. This time is the wave adjustment timescale τ_w for this problem.

However, the thermocline is not yet fully adjusted. As seen in the bottom panels of Figs. 4 and 5, it continues to deepen at a finite rate. This phase can be described in purely advective terms and is associated with the timescale τ_d described in the previous section: water is upwelled and warmed at a rate that depends on the local depth of the thermocline and the strength of the upwelling (Boccaletti et al., 2004a,b). As the thermocline becomes deeper, the size of the cold tongue is reduced, and the heat flux decreases. The process continues until the magnitude of the net surface heat flux equals the amount of heat diffused to the abyss. At that point, only mixing is left which operates on a timescale proportional to κ .

Three different diabatic processes (surface heating with timescale proportional to α , diabatic upwelling with timescale τ_d , and diffusion with timescale proportional to κ) and one dynamical process (wave adjustment with timescale τ_w) operate on remarkably different timescales. The diabatic processes identified by α , τ_d and κ are ultimately responsible for heat entering the basin, while the wave adjustment is responsible for the redistribution of water mass within the basin.

By integrating over the whole basin, we can identify the rate at which heat enters the ocean and we can define an e-folding timescale T given by

$$T^{-1} = \left(\frac{1}{H} \frac{dH}{dt} \right) = \frac{Q}{H} \quad (6)$$

where H is the heat content of the ocean and Q is the total heating at the surface. The e-folding timescale of each diabatic process can then be estimated.

The surface heating leads to an e-folding timescale of $T^{-1} \sim (\alpha/\rho_0 C_p) \Delta T / H_0 T_c$, where H_0 is the depth of the basin, and T_c is the temperature of the abyssal water (to first approximation the total heat content does not change much, so the denominator of Eq. (6) can be substituted with the initial heat content). For $H_0 = 5000$ m, $\Delta T \sim 15^\circ\text{C}$, $T_c \sim 10^\circ$ and $(\alpha/\rho_0)C_p \sim 10^{-5}$ m/s, we get $T \sim 3 \times 10^8$ s. The upwelling process has a timescale τ_d , so that by using Eqs. (3) and (4), an e-folding timescale can be derived $T^{-1} \sim \tau_d^{-1} D \Delta T / H_0 T_c = w_e h \Delta T / H_0 T_c D$. For $w_e \sim 0.5 \times 10^{-5}$ m/s, $h \sim 50$ m and a thermocline depth on the order of 150 m, $T \sim 2 \times 10^9$ s. Finally, diffusion will produce an e-folding timescale of $T \sim \kappa \Delta T / D H_0 T_c$ which for $\kappa \sim 10^{-6}$ m²/s gives $T \sim 2 \times 10^{10}$ s.

Fig. 7 shows the e-folding timescale for the numerical simulation compared with the estimates above. For the first month, heat enters at a rate that depends on surface processes alone. After the first month, the heating slows down to an e-folding timescale similar to that estimated for the upwelling process. Finally, after about a decade, the e-folding timescale is clearly diffusive. As the abyss warms up, the heat content of the ocean increases and the e-folding timescale becomes even longer.

In due course, the entire fluid will be at a uniform temperature of 25°C , and diffusion is responsible for the final homogenization. In the particular case of Fig. 7, the background

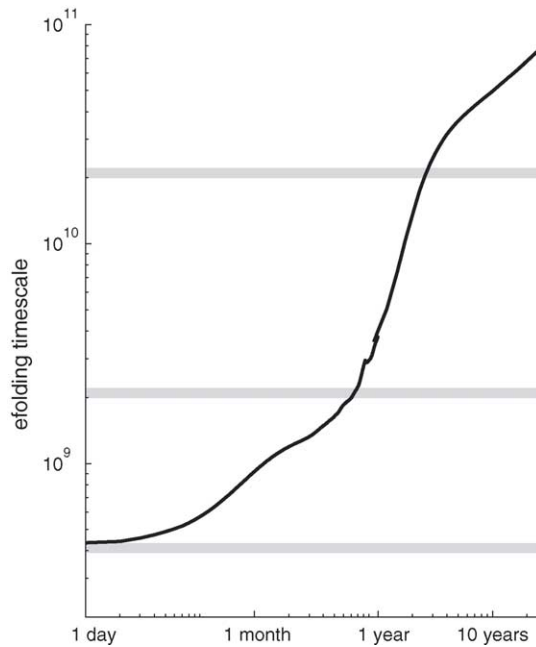


Fig. 7. Log–log plot of the e-folding timescale of the heat content evolution ($\partial H/H$, values in seconds). The gray lines are estimates of the e-folding timescales associated with diabatic processes. The top line is an estimate for diffusive processes; the middle line is an estimate for upwelling processes; the bottom line is an estimate for surface heating.

diffusivity was chosen to be small ($0.01 \times 10^{-4} \text{ m}^2/\text{s}$). However, for larger values of diffusivity, the distinction between mixing and wind-driven deepening is going to be blurred, as the two timescales associated with those processes get closer. Fig. 8 shows a number of examples for different values of diffusivity. The timescale separation is critically dependent on the choice of diffusivity. For large mixing, even at these early stages, the thermocline deepens and widens at approximately the same rate, so that it is difficult to separate these two processes. As diffusivity is decreased, the effect of mixing becomes secondary in the first few decades of the adjustment as surface heating in the cold tongue dominates the increase in heat content of the basin. It is therefore critical to realize that the distinction between τ_d and diffusive timescales is only possible in cases in which diffusion is small. Coarse resolution models, which typically have high diffusivity values, are an important example in which this distinction might be lost.

The fact that purely dynamical processes such as wave adjustment are not enough to determine the solution is implicitly acknowledged in theories for the thermocline by the presence of an arbitrary stratification along the eastern boundary, necessary to close the problem (Luyten et al., 1983). That arbitrary stratification is a measure of the heat content of the ocean, which must be determined by diabatic processes. Because in this experiment, no global constraint exists on the heat budget at the surface—other than the fact that eventually surface temperatures must be 25°C everywhere—the thermocline keeps deepening and

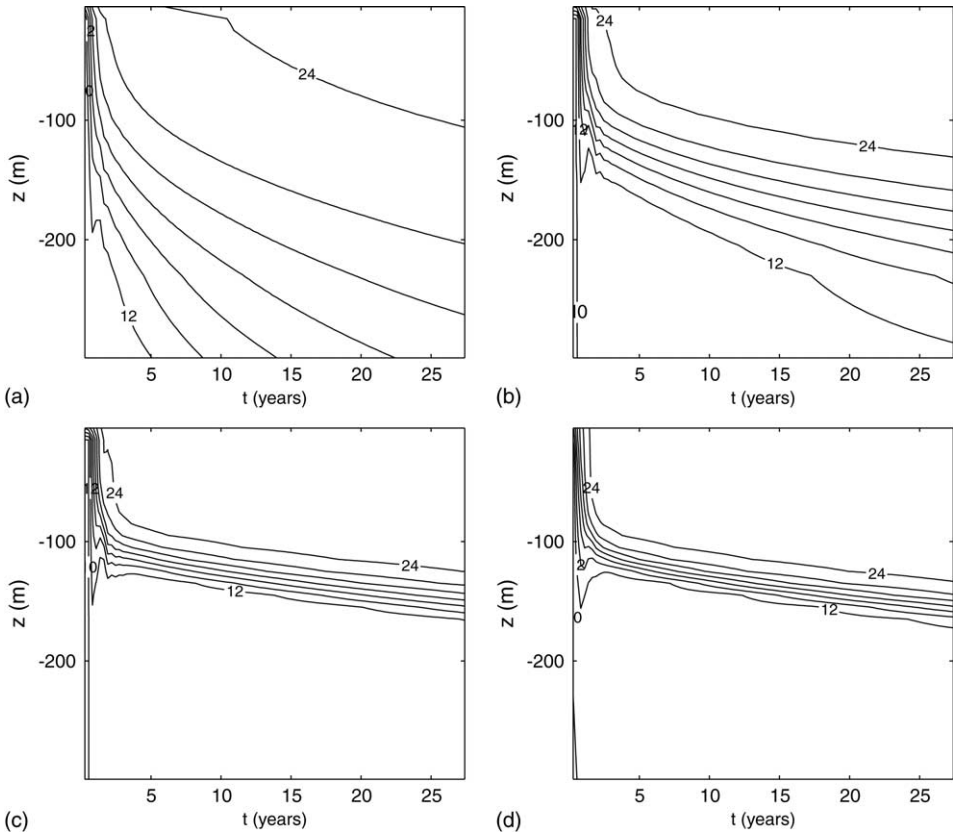


Fig. 8. Separation of τ_d and τ_k ; evolution of the thermocline at 20° longitude, at the equator, for different values of diffusivity: (a) $\kappa = 1 \times 10^{-4} \text{ m}^2/\text{s}$; (b) $\kappa = 0.1 \times 10^{-4} \text{ m}^2/\text{s}$; (c) $\kappa = 0.01 \times 10^{-4} \text{ m}^2/\text{s}$; (d) Pacanowski–Philander mixing scheme (Pacanowski and Philander, 1981).

dissolving, until the basin is completely isothermal. We shall see in the next section that when a more stringent condition is set on the heat budget, the thermocline depth is finite and determined.

5. Heating, cooling and communication

In the previous section, we have analyzed the timescales involved in the formation (and ultimately dissipation of) a thermocline formed while heating a basin initially at 10°C towards 25°C . We shall now show how, in the case of small diffusivity, wind-driven diabatic processes dominate the timescale for adjustment to equilibrium. In order to do this, we turn to the following problem. Assume that the same initially isothermal basin is subject to a restoring boundary condition, where T^* is 25°C in the tropics between 12°S and 12°N , and linearly tapers poleward of 12° latitude to 10°C at the boundaries. The steady state of this

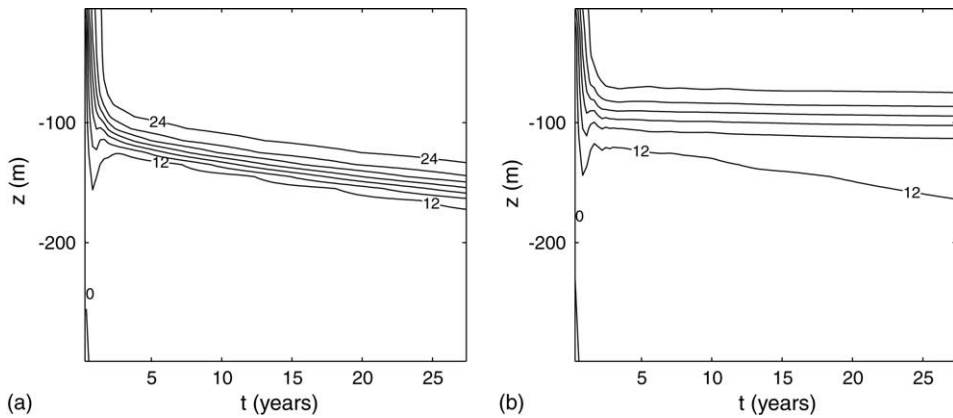


Fig. 9. Comparison of the adjustment at 20° longitude, on the equator, between the case with no cooling (a) and the case with cooling (b).

model is shown in Fig. 1, and was used for the linear perturbation problem. How does the model reach that equilibrium state?

The change in thermal boundary condition has a profound effect on the final solution and therefore on the adjustment process. Fig. 9 compares the evolution of the thermocline at the equator for the case in which surface temperatures are restored to a uniform 25°C (previous section) and for the current case with high latitude cooling. In the previous case, the thermocline is rapidly formed, but then continues to deepen and, eventually, dissolves. In the case of high latitude cooling, the thermocline is formed according to the same dynamics, but is then constrained into place.

The dynamical adjustment in the presence of cooling is almost identical to the case of the previous section. An initial warm layer is redistributed by a frontal adjustment similar to the one shown in Fig. 6. However, unlike the previous case, cooling is immediately established at the poleward boundaries, which disposes off the warm water brought in from the tropics by Ekman transport. As before, wave adjustment occurs in just a few months, followed by an advective deepening of the thermocline. The thermocline deepens, progressively reducing the heating, and leading towards a balanced heat budget.

Fig. 10 shows the mean surface heatfluxes divided into cooling and warming for this last experiment. The cooling is established almost immediately, as it is primarily due to Ekman transport into a region of cold restoring. The heating, on the other hand, adjusts more slowly. The main diabatic process at work here is that connected to the wind-driven circulation, as indicated by the timescale over which the deepening occurs, consistent with the estimate of Eq. (5).

Diffusion is still acting on the thermocline at the end of the adjustment, and induces a circulation with upwelling under the thermocline, surface poleward flow, and deep return flow. The strength of this circulation is directly dependent on diffusivity (Bryan, 1987; Huang, 1999; Boccaletti et al., 2004a,b), and because diffusivity is small, it is weak. Although diffusion acts for a long time, it does not significantly alter the depth of the tropical thermocline, as the diffusively driven circulation does not contribute much to the heat budget.

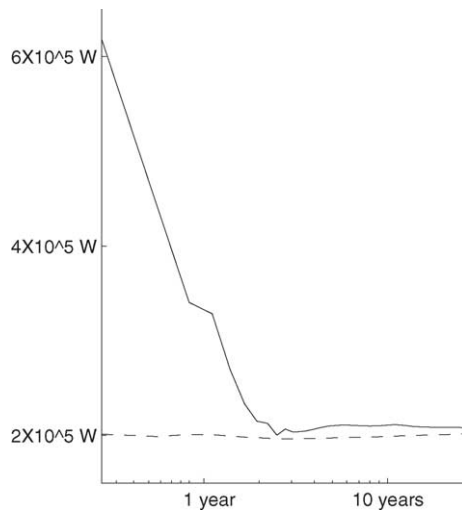


Fig. 10. Evolution of heating (solid) and cooling (dashed) for the last experiment. For convenience, the cooling is multiplied by -1 .

Calculations were run for much longer to verify that the solution would not be qualitatively different. While the abyss warms up, the main thermocline is locked in place by the dominant wind-driven heat budget.

The conclusion that can be drawn from this set of experiments is that the heat budget constrains the depth of the thermocline, as proposed in Boccaletti et al. (2004a,b), and it does so on a timescale associated with the dominant diabatic process, which is fast and wind-driven.

6. Discussion and conclusions

How long does it take for the thermocline to respond to a surface perturbation? What timescale is associated with the background stratification of the upper ocean? These two questions are often considered as distinct. For the former, Gu and Philander (1997) invoked an adiabatic timescale, associated with advection of anomalies. For the latter, the long-term effects of open-ocean turbulent diffusion are invoked to explain diabatic changes in the mean state of the ocean (Tziperman, 1986; Huang, 1991). Therefore, the assumption is that gross structure of the thermocline must be determined over diffusive timescales, while short-term changes are governed by adiabatic dynamics.

In this paper, we have recast these questions from the perspective of the oceanic heat budget. In this framework, the two are clearly linked. We have identified a diabatic process associated with wind-driven upwelling, which is responsible, in the limit of small diffusion, for the timescale τ_d of both.

When an existing thermocline is perturbed, the perturbation excites a dynamical response expressed in terms of waves propagating around the basin. This adjustment is associated with

a timescale which is faster than the time it takes for the ocean to reach a new equilibrium. The latter depends instead on the rate at which the thermocline can change its absolute depth, or—in other words—the rate at which the volume of warm water can change. This rate depends on the strength of wind-driven upwelling and on surface heating and determines the adjustment timescale τ_d .

This same timescale is relevant for the formation of the thermocline. When mechanical and thermal forcing are applied to an isothermal basin, the surface temperature initially increases on a timescale proportional to α^{-1} . Off the equator, a zonally symmetric meridional circulation is established, which is however incompatible with the no-flow boundary conditions. A front travels around and across the basin to satisfy boundary conditions and redistribute mass. After this dynamical adjustment, the heat budget *is not*, in general, balanced. Two cases of interest were shown in this instance: one in which no cooling was present and one in which warming and cooling had to balance.

In the case of heating and cooling, an approximately balanced heat budget is reached on the order of years, through this mechanism. Once the upper ocean has reached equilibrium, diffusion acts to equilibrate the abyss and the unventilated part of the thermocline. For low values of diffusivity, the heat budget is almost entirely balanced after τ_d , and the residual diffusive effects have small consequences on the absolute depth of the thermocline. Observed values of mixing in the ocean suggest that we might be close to the case of low diffusivity (Ledwell et al., 1993), making the timescale τ_d of central importance for the variability of the mean state of the ocean.

The wind-driven circulation simulated by the model in these experiments has consisted almost entirely of an overturning cell driven by Ekman flow. Much of the heat transported out of the tropics in the real ocean is carried by a similar circulation (Klinger and Marotzke, 2000). However, the western boundary current, which was not simulated in the small basin runs, is also responsible for a large heat transport and it is dynamically very different from that of the simpler Ekman flow. In particular, the boundary current is directly dependent on the baroclinic adjustment of the entire basin (Anderson and Gill, 1975). A full exploration of the role of the boundary current in the global heat budget is well beyond the scope of this paper. If the heat transport is primarily accomplished by the Ekman flow, as suggested by Klinger and Marotzke (2000), then the cooling is just the result of surface Ekman flow entering a region of colder temperatures, and is largely independent of the dynamical adjustment of the thermocline.

If, on the other hand, the heat transport is accomplished by the boundary current, the cooling that results is sensitive to adjustments in the structure of the main thermocline, leading to a more complicated relation between dynamical adjustment and heat budget. More work is needed to identify what controls the diabatic timescale in this more complicated scenario. Furthermore, the size of the basin was chosen to be small to allow for relatively short integrations. In a larger basin, the timescale of the wave adjustment τ_w increases, introducing a further lag in the adjustment process. While this lag does not ultimately change the fact that thermocline formation must be controlled by diabatic processes, it can affect the overall response time to a perturbation. Full exploration of this issue is beyond the scope of this paper, but the reader is referred to Boccaletti et al. (2004a,b) for further considerations on the problem.

When diffusion is small, the diffusive timescale is long. However, because the heat transport due to diffusion is small, the dominant process controlling the heat budget is wind-driven, and diabatically equilibrates the basin over a time τ_d . Because τ_d is on the order of years to decades at most, it may play a critical role in the observed decadal variability of the tropical thermocline (Mantua et al., 1997). This mechanism is considerably different from that explored by Gu and Philander (1997). Investigation of this issue is taken up in Boccaletti et al. (2004a,b).

Acknowledgments

The author wishes to thank George Philander, Alexey Fedorov, Robert Hallberg, Geoff Vallis, Kirk Bryan and two anonymous reviewers for useful comments at different stages of this work. Early ideas for these experiments were first discussed with Anthony Rosati, who is gratefully acknowledged. Particular gratitude goes to Ronald C. Pacanowski who helped with the simulations shown in this study and with many more not shown. The support of NASA fellowship NGT5-30333 is acknowledged.

References

- Anderson, D.L.T., Gill, A.E., 1975. Spin-up of a stratified ocean, with applications to upwelling. *Deep-Sea Res.* 22, 583–596.
- Boccaletti, G., Pacanowski, R.C., Philander, S.G.H., 2004. A diabatic mechanism for decadal variability, *Dyn. Atmos. Oceans*, in this issue.
- Boccaletti, G., Pacanowski, R.C., Philander, S.G.H., Fedorov, A.V., 2004b. The thermal structure of the upper ocean. *J. Phys. Oceanogr.* 34, 888–902.
- Bryan, F., 1987. Parameter sensitivity of Primitive Equation Ocean General-Circulation Models. *J. Phys. Oceanogr.* 17, 970–985.
- Cane, M.A., 1989. A mathematical note on Kawase's study of the deep-ocean circulation. *J. Phys. Oceanogr.* 19, 548–550.
- Cane, M.A., Sarachik, E.S., 1979. Forced baroclinic ocean motions, III: the linear equatorial basin case. *J. Mar. Res.* 37, 355–398.
- Deser, C., Blackmon, M.L., 1995. On the relationship between tropical and North Pacific sea surface temperature variations. *J. Climate* 8, 1677–1680.
- Fine, R.A., Peterson, W.H., Ostlund, H.G., 1987. The penetration of tritium into the tropical Pacific. *J. Phys. Oceanogr.* 17, 553–564.
- Godfrey, J.S., 1975. On ocean spindown I: a linear experiment. *J. Phys. Oceanogr.* 5, 399–409.
- Griffiths, R.W., 1986. Gravity currents in rotating systems. *Ann. Rev. Fluid Mech.* 18, 59–89.
- Gu, D., Philander, S.G.H., 1997. Interdecadal climate fluctuations that depend on exchanges between the tropics and the extratropics. *Science* 275, 805–807.
- Haney, R.L., 1971. Surface thermal boundary condition for Ocean Circulation Models. *J. Phys. Oceanogr.* 1, 241–248.
- Hazeleger, W., Visbek, M., Cane, M., Karspeck, A., Naik, N., 2001. Decadal upper ocean temperature variability in the tropical Pacific. *J. Geophys. Res.* 106, 8971–8988.
- Hellfrich, K.R., Kuo, A.C., Pratt, L.J., 1999. Nonlinear Rossby adjustment in a channel. *J. Fluid Mech.* 390, 187–222.
- Huang, R.X., 1991. The three-dimensional structure of wind-driven gyres: ventilation and subduction. *Rev. Geophys. (Suppl.)*, 590–609.

- Huang, R.X., 1999. Mixing and energetics of the oceanic thermohaline circulation. *J. Phys. Oceanogr.* 29, 727–746.
- Johnson, H.L., Marshall, D.P., 2002. A theory for the surface Atlantic response to thermohaline variability. *J. Phys. Oceanogr.* 32, 1121–1132.
- Kawase, M., 1987. Establishment of deep circulation driven by deep-water production. *J. Phys. Oceanogr.* 17, 2294–2317.
- Klinger, B.A., Marotzke, J., 2000. Meridional heat transport by the subtropical cell. *J. Phys. Oceanogr.* 30, 696–705.
- Ledwell, J.R., Watson, A.J., Law, C., 1993. Evidence for slow mixing across the pycnocline from an open-ocean tracer-release experiment. *Nature* 364, 701–703.
- Luyten, J.R., Pedlosky, J., Stommel, H., 1983. The ventilated thermocline. *J. Phys. Oceanogr.* 13, 292–309.
- Lysne, J., Chang, P., Griese, B., 1997. Impact of the extratropical Pacific on equatorial variability. *Geophys. Res. Lett.* 21, 2589–2592.
- Mantua, N.J., Hare, S.R., Zhang, Y., Wallace, J.M., Francis, R.C., 1997. A Pacific decadal climate oscillation with impacts on salmon. *Bull. Am. Met. Soc.* 78, 1069–1079.
- McPhaden, M.J., Fine, R.A., 1988. A dynamical interpretation of the tritium maximum in the central equatorial Pacific. *J. Phys. Oceanogr.* 18, 1454–1458.
- Pacanowski, R.C., Philander, S.G.H., 1981. Parameterization of vertical mixing in numerical models of tropical oceans. *J. Phys. Oceanogr.* 11, 1443–1451.
- Philander, S.G.H., 1990. *El Niño, La Niña and the Southern Oscillation*. Academic Press.
- Schneider, N., Venzke, S., Miller, A.J., Pierce, D.W., Barnett, T.P., Deser, C., Latif, M., 1999. Pacific thermocline bridge revisited. *Geophys. Res. Lett.* 26, 1329–1332.
- Stern, M.E., 1980. Geostrophic fronts, bores, breaking and blocking waves. *J. Fluid Mech.* 99, 687–703.
- Tziperman, E., 1986. On the role of interior mixing and air–sea fluxes in determining the stratification and circulation of the oceans. *J. Phys. Oceanogr.* 16, 680–693.
- Yang, J., 1999. A linkage between decadal climate variations in the Labrador Sea and the tropical Atlantic. *Geophys. Res. Lett.* 26, 1023–1026.